



HAL
open science

Von Willebrand factor: how unique structural adaptations support and coordinate its complex function

Peter J. Lenting, Cécile Denis, Olivier Christophe

► To cite this version:

Peter J. Lenting, Cécile Denis, Olivier Christophe. Von Willebrand factor: how unique structural adaptations support and coordinate its complex function. *Blood*, 2024, 144 (21), pp.2174-2184. 10.1182/blood.2023023277 . hal-04817254

HAL Id: hal-04817254

<https://hal.science/hal-04817254v1>

Submitted on 3 Dec 2024

HAL is a multi-disciplinary open access archive for the deposit and dissemination of scientific research documents, whether they are published or not. The documents may come from teaching and research institutions in France or abroad, or from public or private research centers.

L'archive ouverte pluridisciplinaire **HAL**, est destinée au dépôt et à la diffusion de documents scientifiques de niveau recherche, publiés ou non, émanant des établissements d'enseignement et de recherche français ou étrangers, des laboratoires publics ou privés.

Von Willebrand factor: how unique structural adaptations support and coordinate its complex function

Peter J Lenting¹, Cécile V Denis¹, Olivier D Christophe¹

¹Université Paris-Saclay, INSERM, Hémostase Inflammation Thrombose HITh U1176, 94276, Le Kremlin-Bicêtre, France

Running title: A closer look at VWF

Corresponding author:

Peter J. Lenting

Inserm U1176

80 rue du Général Leclerc

94276 Le Kremlin-Bicetre

France

Tel: +331 49 59 56 00

Abstract: 238 words

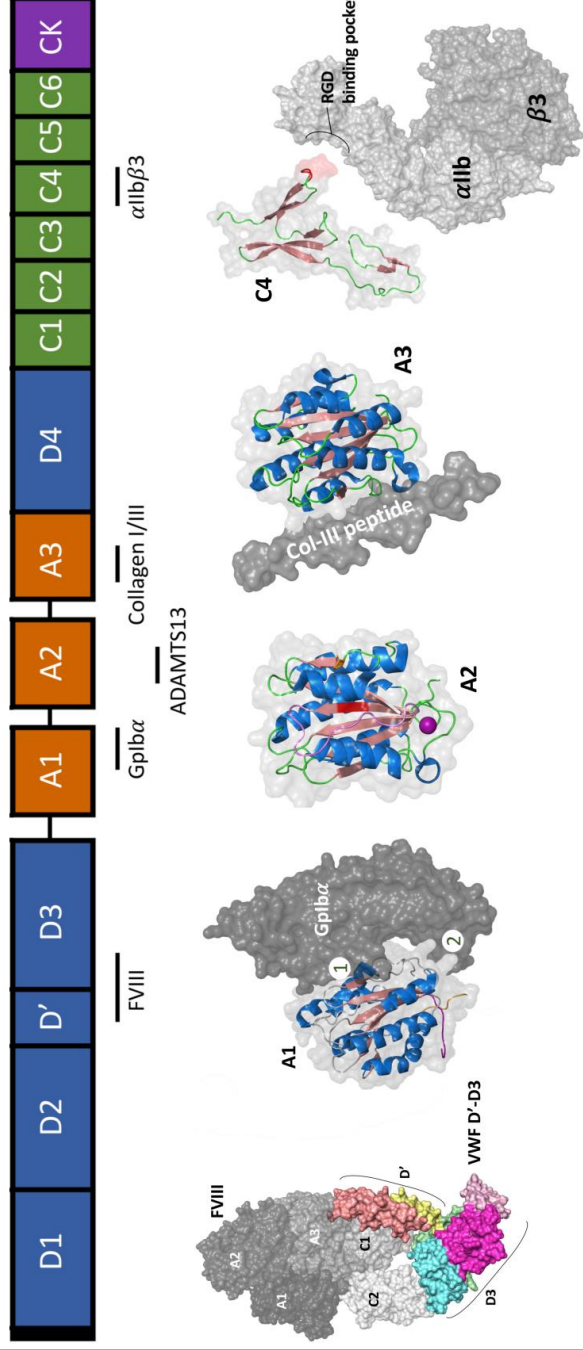
Main text: 3991 words

Figures: 6

References: 100

PJL, CVD and ODC designed and wrote the manuscript.

A closer look at von Willebrand factor structure



Von Willebrand factor (VWF) binds multiple ligands, the interactions of which are regulated differently for each of these ligands. Ligand binding is supported and coordinated via unique structural adaptations in the domains that constitute VWF.

Abstract

Von Willebrand factor (VWF) is a multimeric protein consisting of covalently linked monomers, which share an identical domain architecture. Although involved in processes like inflammation, angiogenesis and cancer metastasis, VWF is mostly known for its role in hemostasis, by acting as a chaperone-protein for coagulation factor VIII (FVIII) and by contributing to the recruitment of platelets during thrombus formation. To serve its role in hemostasis, VWF needs to bind a variety of ligands, including FVIII, platelet-receptor glycoprotein Ib-alpha, VWF-cleaving protease ADAMTS13, sub-endothelial collagen and integrin alpha-IIb/beta-3. Importantly, interactions are differently regulated for each of these ligands. How are these binding events accomplished and coordinated? The basic structures of the domains that constitute the VWF protein are found in hundreds of other proteins of pro- and eukaryotic organisms. However, the determination of the three-dimensional structures of these domains within the VWF context and especially in complex with its ligands reveals that exclusive, VWF-specific structural adaptations have been incorporated in its domains. They provide an explanation of how VWF binds its ligands in a synchronized and timely fashion. In the current review, we have focused on the domains that interact with the main ligands of VWF and discuss how elucidating the three-dimensional structures of these domains has contributed to our understanding of how VWF function is controlled. We further detail how mutations in these domains that are associated with von Willebrand disease modulate the interaction between VWF and its ligands.

Introduction

Von Willebrand factor (VWF) is among the largest proteins circulating in plasma. Although recognized to participate in processes like inflammation, angiogenesis and cancer metastasis, VWF is predominantly known for its role in hemostasis.¹⁻³ Indeed, its deficiency or dysfunction is associated with bleeding complications in a disorder known as von Willebrand disease (VWD).⁴ VWF is synthesized as a single-chain polypeptide with a distinct domain structure: D1-D2-D'D3-A1-A2-A3-D4-C1-C2-C3-C4-C5-C6-CK (with CK referring to cysteine knot domain; Figure 1).⁵ Post-translational processing includes the removal of the D1-D2 region (also known as the VWF propeptide), and the generation of heterogeneously-sized multimers via the formation of inter-molecular disulfide bridges in the C-terminal CK-domain and the N-terminal D'D3-region.⁶

Regarding its role in hemostasis, VWF will need to interact with various ligands, including coagulation factor VIII (FVIII), platelet-receptor glycoprotein Ib α (GpIb α), VWF-cleaving protease ADAMTS13, sub-endothelial collagen and integrin α IIb β 3 (Figure 1).¹ Importantly, the interaction with each of these ligands is regulated in a different manner. For instance, whereas VWF should bind FVIII with high affinity in the circulation, it needs to avoid interacting with GpIb α until platelet recruitment becomes relevant. The beauty of the VWF molecule is that the keys to unlock different levels of regulation are directly present in its structure. At first glance, the domains that compose VWF are not unique, since the general folding of the A-, C-, CK-, and D-domains can be found in many proteins in pro- and eukaryotic organisms. However, several distinct adjustments have been incorporated into the VWF structure to meet the necessary requirements regarding ligand-specific interactions. The most "famous" adaptation is the unusually large size of VWF. Its large size makes VWF susceptible to conformational changes under influence of hydrodynamic forces, which is one mechanism to control VWF function.^{7,8}

When reviewing VWF structural studies performed over the last two decades, the secrets of this fascinating molecule have slowly been unraveled, helping us to recognize how complexation between VWF and its ligands is regulated. In this review, we will therefore concentrate on the main ligands of VWF and discuss how elucidating the three-dimensional structures of VWF domains, generally in complex with its ligands, has contributed to our understanding of how VWF function is controlled. In addition, these insights also improved our knowledge on why certain mutations are associated with VWF dysfunction and subsequent bleeding tendencies.

FVIII binding to the D'D3-region

VWF contains four full D-assemblies and another partial one, which together encompass near 60% of the total amino acid content. A closer look at these D-assemblies has revealed the presence of four distinct structures: a von Willebrand D (VWD)-domain, a C8-fold, a trypsin inhibitor-like (TIL)-structure and an E-module.⁵ These structures can be found in the D1, D2, D3 and D4-assemblies, while the D'-segment contains only the TIL-structure and the E-module. Two of the D-assemblies, *i.e.* the D'D3-region (residues Ser⁷⁶⁴-Thr¹²³³), are located N-terminally in the mature subunit and contribute to the multimerization process by making inter-subunit cysteine bonds with a D'D3-region of another VWF molecule.^{5,9-11} Besides its role in VWF multimerization, the D'D3-region is also critical to the

interaction between VWF and FVIII.¹² VWF is a necessary chaperone-protein for FVIII, protecting it from rapid clearance and proteolytic degradation. Indeed, the absence of VWF is associated with strongly reduced FVIII levels.¹³ Expression of the dimeric D'D3 portion in VWF-deficient mice fully normalized FVIII levels, showing that this region harbors all the information to bind FVIII.¹⁴ Notably, the affinity of the FVIII/VWF interaction is unusually high ($K_D \approx 0.5$ nM), allowing >95% of FVIII to circulate complexed with VWF.^{13,15-17}

Although classic mutagenesis studies identified amino acids involved in FVIII binding¹⁸⁻²¹, the availability of FVIII and VWF structures has provided detailed insight into their interaction. First, in two back-to-back publications, Chiu *et al.* and Yee *et al.* used negative-stain and single-particle electron microscopy to generate low-resolution images of the complex between FVIII and D'D3.^{22,23} They showed that the FVIII light chain ($\alpha 3$ -A3-C1-C2) is enveloped by the D'D3 region, with the D3-assembly interacting with the C1-C2 domains and the D'-segment binding to the $\alpha 3$ -A3 portion. Another study confirmed the relevance of the D'-segment in binding FVIII, and used hydrogen-deuterium exchange mass spectrometry and mutational analysis to identify the D' Arg⁷⁸²-Cys⁷⁹⁹ segment as part of the FVIII-binding interface.²⁴ A comprehensive view of the D'D3/FVIII complex was obtained by using a FVIII-D'D3 fusion protein, designated BIVV001 (now renamed efanesoctocog alfa).²⁵ By combining cryo-electron microscopy and existing structures of FVIII and the D'D3 region, a high resolution (2.9 Å) visualization of the D'D3/FVIII complex was generated (Figure 2A-B). The substructures of the D'D3 are distinguishable, with the C8-3-fold binding to the bottom of the FVIII C2-domain, and the VWD-3-domain to the FVIII C1-domain. Furthermore, the TIL'-structure interacts with the FVIII C1- and A3-domains, including the acidic $\alpha 3$ -region. More specifically, the acidic FVIII residues Asp¹⁶⁷⁶, Asp¹⁶⁷⁸ and Asp¹⁶⁸¹ interact with TIL'-residues Arg⁸²⁰, Arg⁸²⁶ and Arg⁷⁶⁸, respectively, while sulfated FVIII residue Tyr¹⁶⁸⁰ interacts directly with TIL'-residue Arg⁸¹⁶ (Figure 2A-B).²⁵

The detailed structure of the D'D3/FVIII complex explains many of the mutations that impair FVIII binding. For example, mutations within VWF in the Arg⁷⁸²-Cys⁷⁹⁹ region and at Arg⁸¹⁶ reduce FVIII binding and are known for their association with VWD-type 2N (Figure 2C).²⁶⁻²⁸

A relevant question is whether FVIII binding dependent on multimerization. Dimeric VWF, which is the only natural VWF species that lacks dimerized N-termini, has a 5-fold lower affinity for FVIII compared to multimeric VWF.²⁹ This suggests that covalent bonding between VWF N-termini enhances FVIII binding. Since VWF-FVIII binding studies comparing preparations enriched in low- and high-molecular weight multimers identified similar affinities for FVIII, additional multimerization does not seem to further improve FVIII binding.¹⁶ Indeed, the FVIII/VWF ratio remains relatively unchanged in patients characterized by a loss of high molecular weight multimers.³⁰

Gplb α binding to the A1 domain

Adjacent to the D'D3-region is the A1-domain (residues Tyr¹²⁷¹-Asp¹⁴⁵⁹), with the N- and C-termini being connected by a disulfide bridge (Cys¹²⁷²-Cys¹⁴⁵⁸). This domain shares structural resemblance with the A2- and A3-domains in a von Willebrand A (VWA)-fold that is widely spread among protein families in eukaryotes and prokaryotes.³¹ The general structure consists of central hydrophobic β -sheets flanked by amphipathic α -helices, making up a Rossmann-like fold (Figure 3A).³² The A1-

domain mediates binding of VWF to the platelet-receptor GpIb α , and its crystal structure was elucidated in the 1990s.^{33,34} Solving the structure of the VWF/GpIb α complex was hampered because both proteins do not interact spontaneously, as their association is shear force-dependent.³⁵ By using fragments containing gain-of-function mutations that facilitate complexation, however, Huizinga *et al.* solved the structure of the A1-domain bound to the N-terminal domain of GpIb α .³⁶ Additional structures of VWF/GpIb α complexes have since been produced using both wild-type and other gain-of-function variants.^{37,38}

The VWF/GpIb α complex involves two main interactive sites, one containing A1-domain helix α 3, loop α 3 β 4 and strand β 3 (interactive site 1) and a second one containing A1-domain loops α 1 β 2, β 3 α 2 and α 3 β 4, located at the bottom face of the A1-domain (interactive site 2) (Figure 3A-B). The structure of the complex revealed insights into how different mutations affect binding between both proteins. First, mutations in the A1-domain or in GpIb α resulting in a loss-of-function (associated with VWD-type 2M or Bernard-Soulier syndrome, respectively) are found within the respective interactive sites.³⁶ Second, gain-of-function mutations in GpIb α known to provoke platelet-type VWD were found within a unique 16-residue β -hairpin conformation that penetrates into interactive site 1 of the A1-domain. In the unbound state, this region adopts a disordered or α -helical state, whereas the β -hairpin structure is favored for VWF binding.^{36,37} Mutations in this region (*eg.* Met²³⁹Val) stabilize the β -hairpin structure, causing spontaneous binding of GpIb α to VWF.

Surprisingly, none of the gain-of-function mutations within the A1-domain associated with VWD-type 2B are located within either interactive site, suggesting that other regions within the A1-domain are involved in regulating GpIb α binding. Insight into the underlying mechanism was obtained when recombinant A1-domain fragments with differently sized flanking peptides were compared for GpIb α binding.^{39,40} The shorter the flanking peptide, the more efficient the A1-domain binds GpIb α . The molecular basis by which the flanking peptides control A1-GpIb α interactions was unraveled by Li and colleagues.⁴¹⁻⁴³ They demonstrated that residues Gln¹²³⁸-His¹²⁶⁸ at the N-terminus of the A1-domain interact directly with residues Leu¹⁴⁶⁰-Asp¹⁴⁷² at the C-terminus of the A1-domain. This structure is referred to as auto-inhibitory module (AIM), and blocks access of GpIb α to interactive site 2 at the bottom of the A1-domain.^{41,42} Under pressure of hydrodynamic forces, the AIM-peptides dissociate, thereby exposing GpIb α -interactive site 2 (Figure 3A-B).⁴³ It is noteworthy that ristocetin, an antibiotic that induces VWF/GpIb α binding, is known to interact with peptides Cys¹²³⁷-Pro¹²⁵¹ and Glu¹⁴⁶³-Asp¹⁴⁷², both of which are contained within the AIM.⁴⁴ It seems conceivable that ristocetin destabilizes the AIM-structure to induce GpIb α binding. Importantly, mutations known to be associated with VWD-type 2B are generally located within or near the AIM and disrupt the interaction between both peptides, providing an explanation for spontaneous binding of these mutants to GpIb α (Figure 3C). Together, these studies show that conformational changes in the immediate surrounding of the A1-domain control its interactions with GpIb α . Interestingly, a number of nanobodies have been described that support this notion. First, Hulstein and colleagues described an A1-domain directed nanobody, named AU-VWFA-11, that only binds VWF in a GpIb α -binding conformation.⁴⁵ This nanobody has been used to determine the active conformation of VWF in a spectrum of diseases.⁴⁶

Another example is caplacizumab, a bivalent nanobody that inhibits VWF-GpIb α interactions, and is approved for treatment of thrombocytopenic thrombotic purpura.^{47,48} A monovalent variant of caplacizumab (designated VHH81) was used to make a co-crystal with the A1-domain. VHH81 binds to and stabilizes the AIM-structure, thereby preventing its dissociation under shear stress (Figure 3B). As such, exposure of interactive site 2, and subsequent GpIb α binding are inhibited.⁴² Another nanobody designated 6D12 also binds to the AIM but has the opposite effect of caplacizumab: 6D12 promotes dissociation of the AIM-peptides, converting VWF into an active GpIb α -binding conformation.⁴³ Apparently, nanobodies are valuable tools to monitor conformational changes in general and in VWF in particular, and another example will be discussed when addressing the VWF A3-domain.

Knowing that shear forces are needed to unblock GpIb α -interactive sites, the question follows whether this process is multimer dependent. In the 1980's, Chopek *et al.* demonstrated that GpIb α -binding is strictly multimer-size dependent, in that low-molecular weight multimers are too small to support GpIb α -dependent platelet adhesion.⁴⁹ This effect is particularly visible in patients displaying impaired multimerization and associated bleeding complications (VWD-type 2A). It is assumed that unfolding of VWF is size-dependent, with larger multimers being more sensitive to hydrodynamic forces than smaller multimers.^{7,8}

ADAMTS13 binding to the A2 domain

The A2-domain (residues Arg¹⁴⁹²-Ser¹⁶⁷¹) plays a specific role in regulating VWF function and multimer size. Structurally, the A2-domain differs from other VWA-domains by lacking the disulfide bridge that connects the N- and C-terminal ends of the domain.⁵⁰ This allows the A2-domain to have a more flexible structure and adapt its conformation when exposed to hydrodynamic forces, a necessary capacity knowing that proteolytic regulation of VWF multimeric size occurs via hydrolysis of the Tyr¹⁶⁰⁵-Met¹⁶⁰⁶ peptide bond by the metalloprotease ADAMTS13.⁵⁰

The crystal structure of the A2-domain revealed a number of relevant differences compared to other members of the VWA-family (Figure 4A).⁵⁰ First, the central α 4-helix is absent in the A2-domain and is replaced by a loop lacking in secondary structure (referred to as α 4-less loop) that is about 6 Å away from the ADAMTS13 cleavage site (Figure 4A). Second, the A2-domain contains a unique vicinal disulfide bond between residues Cys¹⁶⁶⁹-Cys¹⁶⁷⁰.⁵⁰ Third, a distinctive Ca²⁺-binding site is present, coordinated by residues in the β 1-sheet (Asp¹⁴⁹⁸), the α 3-helix (Asp¹⁵⁹⁶, Arg¹⁵⁹⁷) and the α 3 β 4-loop (Ala¹⁶⁰⁰, Asn¹⁶⁰²) (Figure 4A).^{51,52} Finally, an unusual *cis*-Pro residue is present at position 1645 (Figure 4A).⁵⁰ Each of these features seems to be a functional adaptation regulating exposure of the Tyr¹⁶⁰⁵-Met¹⁶⁰⁶ cleavage site. Regarding the α 4-less loop, it reduces access of ADAMTS13 to the scissile bond in the folded state, while its flexible nature allows it to promptly move away from Tyr¹⁶⁰⁵-Met¹⁶⁰⁶ during unfolding of the A2-domain.⁵⁰ Simultaneously, this loop may refold back over the β 4-strand less rapidly than when it would have been an α -helix structure, leaving sufficient time for ADAMTS13 to cleave its target.⁵⁰ Also the *cis*-Pro¹⁶⁴⁵ is suspected to delay refolding of the A2-domain.⁵⁰ The vicinal disulfide bond adds rigidity to the C-terminal end of the A2-domain, increasing the energetic barrier for the domain to unfold. Similarly, the Ca²⁺-site contributes to the stability of the

A2-domain structure, resulting in further resistance to unfolding.^{51,52} Removing the Ca²⁺-binding site or the vicinal disulfide bridge indeed provoke premature unfolding and increased sensitivity to proteolysis by ADAMTS13.^{52,53} In contrast, introducing an artificial covalent connection between the β 1- and β 2-sheets impairs unfolding and prevents ADAMTS13-mediated proteolysis.⁵⁴

Once unfolded, the A2-domain contains an extended interactive site for several domains that are contained within ADAMTS13. In fact, the complete interaction interface extends beyond the A2-domain and also involves regions within the D4-CK fragment of VWF⁵⁵, an aspect which will not be discussed in this review. Within the unfolded A2-domain, the β 4-sheet residues Leu¹⁶⁰³-Met¹⁶⁰⁶ are accessible for the active site of the ADAMTS13 metalloprotease domain, permitting hydrolysis of the Tyr¹⁶⁰⁵-Met¹⁶⁰⁶ scissile bond.^{56,57} For this process to proceed efficiently, the α 4-less loop residues Asp¹⁶¹⁴-Asp¹⁶²² interact with the Disintegrin-domain, the α 5-helix/ β 6-sheet region Ile¹⁶⁴²-Ile¹⁶⁵¹ binds to the Cysteine-rich domain and the α 6-helix residues Glu¹⁶⁶⁰-Arg¹⁶⁶⁸ associate to the Spacer-domain of ADAMTS13 (Figure 4B).^{56,57}

Given the strict control of the A2-domain conformation, it is unsurprising that this regulation can be disturbed by a wide range of mutations (Figure 4C). For example, some mutations will promote exposure of the otherwise buried cleavage site (such as Met¹⁵²⁸Val or Glu¹⁶³⁸Lys), whereas others will delay refolding of the A2-domain (e.g. Arg¹⁵⁹⁷Trp), prolonging the time that ADAMTS13 can cleave the Tyr¹⁶⁰⁵-Met¹⁶⁰⁶ bond.⁵⁸ These mutations ultimately result in increased ADAMTS13-mediated VWF degradation and are referred to as group 2 VWD-type 2A mutations. Patients carrying such mutations display a loss of high-molecular weight multimers and an increased risk of bleeding. Increased VWF degradation is also common in VWD-type 2B.⁵⁹

VWF degradation is further enhanced upon binding of FVIII or Gplb α , suggesting that these ligands modulate the unfolding or refolding of the A2-domain.^{60,61} The susceptibility to ADAMTS13-mediated proteolysis is multimer-size dependent. Larger multimers unfold more easily than smaller multimers when exposed to irregular flow, allowing ADAMTS13 to attack the proteolysis site.^{7,8} This feature is particularly visible in patients manifesting disturbed blood flow, eg. in patients with severe aortic stenosis or those receiving mechanical circulatory support. These patients are often characterized by increased VWF degradation, with a visible loss of the high-molecular weight multimers.^{62,63}

Collagen binding to the A3-domain

The A3-domain spans residues Pro¹⁶⁸⁴-Ser¹⁸⁷³, containing a disulfide bridge that connects the N- and C-terminus of this domain (Cys¹⁶⁸⁶-Cys¹⁸⁷²). The A3-domain mediates binding to collagen types I and III.⁶⁴ The crystal structure of the A3-domain was solved independently by two groups, allowing them to confirm the typical VWA-fold with alternating α -helices and β -sheets.^{65,66} A potential collagen binding site involving the β 3-sheet and the α 2- and α 3-helices was identified via extensive mutational analysis.⁶⁷ The identification of the exact collagen interactive site was facilitated when a collagen III-peptide was identified that specifically binds to VWF.⁶⁸ This peptide was used to generate a co-crystal containing the A3-domain/collagen peptide complex (Figure 5A-B).⁶⁹ The collagen peptide indeed binds to the region encompassing the β 3-sheet and the α 2/ α 3-helices, covering a surface of about 24 Å wide and 30 Å long. In total, 14 amino acids within the A3-domain have been identified to directly

interact with the collagen peptide.⁶⁹ Analysis of the complex also allowed identification of complementary amino acids in collagen I and III involved in binding to VWF. Particularly, the structure has helped to explain why both collagen I and III are able to bind VWF at the same site despite their structural differences (for details see⁶⁹).

Unexpectedly, only 2 patient mutations have been identified that are directly within the interactive surface: Val¹⁷⁶⁰Ile and Arg¹⁷⁷⁹Leu, although it has not specifically been reported whether these mutations indeed affect collagen binding. Patient mutations that have been described to modulate collagen binding are actually outside this surface (Leu¹⁶⁹⁶Arg, Ser¹⁷³¹Thr, Trp¹⁷⁴⁵Lys, Ser¹⁷⁸³Ala, His¹⁷⁸⁶Asp and Pro¹⁸²⁴His) (Figure 5C).⁷⁰⁻⁷⁴ The underlying mechanism by which they impair collagen binding is yet unclear, but may be related to an indirect disturbance of the collagen binding surface.

Binding to collagen resembles that to Gplb α in that larger multimers are more efficient in collagen binding compared to smaller multimers.⁷⁵ In contrast, collagen binding differs from Gplb α binding because it may occur already under static conditions, indicating that the A3-domain does not require shear-induced conformational changes to expose its collagen binding site. Does this mean that the A3-domain is rather static in terms of conformation? Probably not, and there are two indications that point in this direction. First, following association of VWF to collagen, the affinity of VWF for FVIII is reduced, resulting in release of FVIII.⁷⁶ Thus, collagen binding via the A3-domain causes structural changes towards the D'D3-region. Second, we recently identified a nanobody (KB-VWF-D3.1), whose binding sites overlaps the collagen binding site (Figure 5B).⁷⁷ Its binding was strictly dependent on the A2-domain being intact, and ADAMTS13-mediated proteolysis was associated with a loss of binding. One potential explanation is that cleavage in the A2-domain induces changes in the adjacent A3-domain, notably the collagen binding site. As such, ADAMTS13 not only modulates collagen binding by reducing multimer size, but also by indirectly modifying the exposure of the collagen binding site.

α IIb β 3 binding to the C4-domain

The C-terminal portion of the mature VWF subunit contains 6 consecutive von Willebrand C (VWC)-domains, also known as chordin-like cysteine-rich domains. Each domain is relatively small compared to the A- and D-domains, containing 68 to 80 residues.⁵ The general VWC-fold comprises two subdomains (SD1 and SD2) that are linked by a disulfide bridge.⁷⁸ SD1 contains 5 anti-parallel β -strands and the SD2-domain contains 2 anti-parallel β -strands, and internal disulfide bridges between β -strands help to stabilize the overall fold of the VWC-module. Indeed, each VWC-domain contains a CxxCxC- and a CCxxC-motif, which mediate the formation of these disulfide bridges.^{5,79}

Although structures of homologous VWC-domains were previously solved⁸⁰⁻⁸², it took until 2019 before the first structure of a VWF C-domain was reported, *ie.* the C4-domain (residues Ser²⁴⁹⁷-Glu²⁵⁷⁷).⁸³ The relevance of solving the structure of the C4-domain is that it contains an RGD-motif that mediates binding of VWF to integrins α IIb β 3 and α V β 3.⁸⁴⁻⁸⁷

As expected, the C4-domain displays a typical VWC-fold characterized by several anti-parallel β -strands in SD1 and SD2 (Figure 6A-B). However, the distribution of the disulfide bridges differs from other instances of the fold. Collagen IIA, Cellular Communication Network Factor-3 and Crossveinless-2 all share five disulfides.⁸³ Four of these are also found in the VWF C4-domain (Figure

6A). However, a conserved disulfide connecting β -strands β II and β III in SD1 of other proteins is not found in the VWF C4-domain, which instead contains a unique disulfide linking strands β I and β II in SD2 (Figure 6A).

A second unique feature is the presence of the RGD-motif in the VWF C4-domain, which is located in the N-terminal portion of the SD1-domain, between the β I'- and β II'-strands. In the majority of VWC-domains, these β -strands are separated by a very short 2-amino acid loop, whereas in the VWF C4-domain this sequence consists of a 10-amino acid hairpin structure, allowing outward exposure of the RGD-motif (Figure 6A-B).⁸³

The continuous exposure of the RGD-site is compatible with the notion that VWF can bind α IIb β 3 under static conditions. In terms of visualization, there is currently no high-resolution co-complex of the C4-domain with α IIb β 3 reported. However, Zhou *et al.* generated low-resolution electron microscopy images of the VWF D4-CK fragment in complex with α IIb β 3.⁵ In these images, α IIb β 3 is perpendicularly bound to the C4-domain, further confirming that the RGD-motif is well-exposed. Nevertheless, the exposure of the RGD is somehow conformation-dependent, illustrated by the finding that mutations within neighboring C-domains have been associated with reduced VWF binding to α IIb β 3.⁸⁸ It seems probable that these mutations perturb the conformation of the RGD-interactive surface.

As for the C4-domain itself, mutations within this domain affecting α IIb β 3 binding are rare, and to the best of our knowledge, only two have been reported: Val²⁵¹⁷Phe and Arg²⁵³⁵Pro (Figure 6C).⁸⁹ These mutations are associated with a mild bleeding tendency, and may be classified as VWD-type 2M. In line with this mild bleeding tendency are the observations that blocking the RGD-motif using a monoclonal antibody or via mutagenesis results in a mild bleeding tendency in mice.^{90,91} Interestingly, detailed analysis of real-time thrombus formation in these mice revealed an increased instability of the thrombus.⁹⁰ This suggests that the VWF/ α IIb β 3 interaction contributes to the stabilization of platelet-platelet interactions, akin to the role of fibrinogen.

In terms of multimerization, it seems that binding of VWF to α IIb β 3 is multimer-size independent. By comparing plasmas from 85 normal subjects and 115 patients with different types of VWD, including type 2A and type 2B, no differences in α IIb β 3 binding were detected.⁹²

Response to shear stress

Conformational changes due to physical forces are key to the control of VWF function. Coiled VWF multimers unfold into an elongated conformation, the extension of which increases with higher shear.^{93,94} However, extension in itself is insufficient to allow binding. For instance, Fu *et al.* observed elongation of VWF at shears between 80 and 480 dyn/cm², whereas Gplb α binding required minimal 720 dyn/cm².⁹³ Apparently, the force needed to break internal interactions between VWF monomers within a single multimer (estimated to be <0.1 pN at 80 dyn/cm²) is lower than the force that is required to unlock the AIM-structure to induce the high-affinity Gplb α -binding conformation (estimated to be 21 pN).⁹³ The forces required for Gplb α binding are also higher compared to the forces needed to unfold the A2-domain, which have been determined to be about 1 pN.⁸ Regarding the other ligands

(FVIII, collagen and α IIb β 3), it seems that shear contributes little to their interaction, since these ligands bind already efficiently under static conditions.

Interestingly, shear does not only contribute to some of the VWF-ligand interactions, but also directs intermolecular self-association, a means to generate longer and thicker VWF fibers. VWF self-association was first reported by Savage et al., who observed that circulating VWF could associate to surface-bound VWF under high shear.⁹⁵ More recently, it was shown that this process is reversible and self-limiting, and requires a minimal shear of 240-480 dyn/cm², lower than what is needed for Gplb α binding.⁹⁶ Apart from shear, other mechanisms also regulate self-association. First, ADAMTS13 will limit self-association via proteolysis of extended VWF multimers.⁹⁷ Second, lipoproteins change the extent to which VWF-multimers can self-associate: low-density lipoproteins enhance self-association, whereas high-density lipoproteins have the opposite effect.^{97,98} Finally, VWF mutations Arg¹⁵⁹⁷Trp (VWD-type 2A) and Val¹³¹⁶Met (VWD-type 2B) are associated with increased self-association.^{99,100}

Conclusion

The generation of high-resolution three-dimensional structures have identified VWF-specific configurations that distinguishes its domains from homologous domain structures in other proteins. These structural adaptations provide VWF with the ability to regulate its interactions with a spectrum of ligands at the sub-molecular level: to bind each ligand at the right time. This tight regulation also makes the VWF protein vulnerable in that it can be perturbed by a wide range of mutations. Indeed, VWD-related mutations are not restricted to a particular hot spot, but dispersed over the whole protein. With the support of novel structural insights, we better understand how each group of mutations may impair VWF function.

So far, the structural studies that we have highlighted in this review have focused on the classic ligands for VWF. However, VWF interacts with a large number of other ligands, including circulating proteins as well as cellular receptors.^{2,3} Currently, we know little about where these ligands exactly bind to VWF and how their binding is regulated. Combining functional studies with the generation of additional three-dimensional structures may help us to better visualize this particular aspect. This is of relevance in view of the notion that there is convincing evidence that VWF functions also beyond hemostasis, and it is important to appreciate how these functions are regulated at the molecular level.

Acknowledgements

We would like to thank Dr. Caterina Casari for her contribution to the design and editing of the manuscript, and Dr. Ivan Peyron in preparation of the figures.

Authorship

PJL, CVD and ODC designed and wrote the manuscript.

Conflict of Interest

PJL, CVD and ODC are inventors on patents related to von Willebrand factor. PJL currently receives research funding to institute from BioMarin, Sobi and Sanofi

Legends

Figure 1: Domain structure of VWF

Structurally defined domain architecture of VWF, based on annotation by Zhou and colleagues.⁵ Depicted are approximate binding sites for the ligands discussed in this review.

Figure 2: Structure of the D'D3/FVIII complex:

Panel A: Three-dimensional representation of the VWF D'D3/FVIII complex derived from PDB-deposit 7KWO.²⁵ Structure was generated using PyMOL-software. *Panel B:* Cartoon impression of the complex, highlighting VWF D'D3 subdomains (adapted from²⁵). Principal interaction interfaces are indicated by arrows. The direct interaction between sulfated FVIII-residue Tyr¹⁶⁸⁰ and VWF D'-residue Arg⁸¹⁶ is shown as well. *Panel C:* Two-dimensional representation of the D'D3 subdomains. Circles indicate positions of residues where mutations have been associated with reduced FVIII binding in patients with von Willebrand disease-type 2N.

Figure 3: Structure of the A1/Gplb α complex:

Panel A: Three-dimensional representation of the VWF A1-domain/Gplb α complex derived from PDB-deposit 1M10.³⁶ N- and C-terminal flanking peptide (N-AIM and C-AIM) are colored in purple and orange, respectively. 1 and 2 refer to interactive sites 1 and 2, respectively. Structure was generated using PyMOL-software. *Panel B:* Three-dimensional representation of the A1-domain in complex with VHH81 (a sequence identical analogue of caplacizumab; pale green) derived from PDB-deposit 7A6O.⁴² VHH81/caplacizumab stabilizes the conformation of the N-AIM/C-AIM interaction, thereby preventing binding of Gplb α to interactive site 1. Structure was generated using PyMOL-software. *Panel C:* Two-dimensional representation of the A1-domain. Circles indicate positions of residues where mutations have been associated with increased Gplb α binding in patients with von Willebrand disease-type 2B. Squares indicate positions of residues where mutations have been associated with reduced Gplb α binding in patients with von Willebrand disease-type 2M. Be aware that in the three-dimensional space, the N- and C-terminal end of the A1 domain are in close vicinity via a disulfide bridge between Cys¹²⁷² and Cys¹⁴⁵⁸.

Figure 4: Structure of the A2-domain:

Panel A: Three-dimensional representation of the VWF A2-domain derived from PDB-deposit 3ZQK.⁵¹ The Tyr¹⁶⁰⁵-Met¹⁶⁰⁶ is in red, the α 4-less loop in violet, the unique Ca²⁺-ion is in purple and cis-Pro¹⁶⁴⁵ in orange. Structure was generated using PyMOL-software. *Panel B:* Cartoon impression the A2-domain in its unfolded conformation. Once unfolded, the A2-domain exposes several interactive sites for ADAMTS13, allowing the Tyr¹⁶⁰⁵-Met¹⁶⁰⁶ scissile bond to be hydrolyzed by the ADAMTS13 metalloprotease domain (MP). Other interactive sites involve the α 4-less loop residues Asp¹⁶¹⁴-Asp¹⁶²² interacting with the Disintegrin domain (Dis), the α 5-helix/ β 6-sheet region Ile¹⁶⁴²-Ile¹⁶⁵¹ binding to the Cysteine-rich domain (Cys) and the α 6-helix residues Glu¹⁶⁶⁰-Arg¹⁶⁶⁸ associating to the Spacer domain of ADAMTS13. *Panel C:* Two-dimensional representation of the A2-domain, including the Ca²⁺ binding site and the vicinal disulfide bridge, both being unique to the A2-domain. The Tyr¹⁶⁰⁵-

Met¹⁶⁰⁶ scissile bond is located in the middle of the β 4-strand. Circles indicate positions of residues where mutations have been associated with increased ADAMTS13-mediated degradation in patients with group 2 von Willebrand disease-type 2A. In contrast to the A1- and A3-domains, the A2-domain lacks a disulfide bridge that connects the N- and C-terminus of this domain.

Figure 5: Structure of the A3-domain/collagen complex:

Panel A: Three-dimensional representation of the VWF A3-domain in complex with a collagen III triple-helical peptide derived from PDB-deposit 4DMU.⁶⁹ Structure was generated using PyMOL-software. *Panel B:* Three-dimensional representation of nanobody KB-VWF-D3.1 docked onto the A3-domain.⁷⁷ The nanobody's binding site overlaps the interactive surface involved in collagen binding. Structure was generated using PyMOL-software. *Panel C:* Two-dimensional representation of the A3-domain. Circles indicate positions of residues where mutations have been associated with reduced collagen binding in patients with von Willebrand disease-type 2M. Note that in the three-dimensional space, the N- and C-terminal end of the A3 domain are in close vicinity via a disulfide bridge between Cys¹⁶⁸⁶ and Cys¹⁸⁷².

Figure 6: Structure of the C4-domain

Panel A: Three-dimensional representation of the VWF C4-domain derived from PDB-deposit 6FWN.⁸³ The RGD-motif is highlighted in red. SD1 and SD2 represent subdomain 1 and 2, respectively. Conserved disulfide bridges (1, 2, 3 & 5) are indicated in blue, and the C4-specific disulfide bridge (C4) is in green. Structure was generated using PyMOL-software. *Panel B:* Provisional alignment (not at scale) of the RGD-motif within the C4-domain (PDB-deposit 6FWN) with the RGD-binding pocket of α IIb β 3 (PDB-deposit 3ZDX). Structure was generated using PyMOL-software. *Panel C:* Two-dimensional representation of the C4-domain. SD1 and SD2 refer to subdomain 1 and 2, respectively. Blue circles indicate disulfide bridges conserved among VWC-domains, whereas green circles represent the disulfide bridge that is unique to the C4-domain. RGD-motif is indicated with red circles. Squares indicate positions of residues where mutations have been associated with reduced α IIb β 3 binding in patients with von Willebrand disease-type 2M.

References

1. Sadler JE. Biochemistry and genetics of von Willebrand factor. *Annu Rev Biochem.* 1998;67:395-424.
2. Lenting PJ, Casari C, Christophe OD, Denis CV. von Willebrand factor: the old, the new and the unknown. *J Thromb Haemost.* 2012;10(12):2428-2437.
3. Atiq F, O'Donnell JS. Novel functions for Von Willebrand factor. *Blood.* 2024. DOI: 10.1182/blood.2023021915
4. Leebeek FW, Eikenboom JC. Von Willebrand's Disease. *N Engl J Med.* 2016;375(21):2067-2080.
5. Zhou YF, Eng ET, Zhu J, Lu C, Walz T, Springer TA. Sequence and structure relationships within von Willebrand factor. *Blood.* 2012;120(2):449-458.
6. Lenting PJ, Christophe OD, Denis CV. von Willebrand factor biosynthesis, secretion, and clearance: connecting the far ends. *Blood.* 2015;125(13):2019-2028.
7. Springer TA. von Willebrand factor, Jedi knight of the bloodstream. *Blood.* 2014;124(9):1412-1425.
8. Zhang X, Halvorsen K, Zhang CZ, Wong WP, Springer TA. Mechanoenzymatic cleavage of the ultralarge vascular protein von Willebrand factor. *Science.* 2009;324(5932):1330-1334.
9. Voorberg J, Fontijn R, van Mourik JA, Pannekoek H. Domains involved in multimer assembly of von willebrand factor (vWF): multimerization is independent of dimerization. *EMBO J.* 1990;9(3):797-803.
10. Katsumi A, Tuley EA, Bodo I, Sadler JE. Localization of disulfide bonds in the cystine knot domain of human von Willebrand factor. *J Biol Chem.* 2000;275(33):25585-25594.
11. Anderson JR, Li J, Springer TA, Brown A. Structures of VWF tubules before and after concatemerization reveal a mechanism of disulfide bond exchange. *Blood.* 2022;140(12):1419-1430.
12. Foster PA, Fulcher CA, Marti T, Titani K, Zimmerman TS. A major factor VIII binding domain resides within the amino-terminal 272 amino acid residues of von Willebrand factor. *J Biol Chem.* 1987;262(18):8443-8446.
13. Pipe SW, Montgomery RR, Pratt KP, Lenting PJ, Lillicrap D. Life in the shadow of a dominant partner: the FVIII-VWF association and its clinical implications for hemophilia A. *Blood.* 2016;128(16):2007-2016.
14. Yee A, Gildersleeve RD, Gu S, et al. A von Willebrand factor fragment containing the D'D3 domains is sufficient to stabilize coagulation factor VIII in mice. *Blood.* 2014;124(3):445-452.
15. Leyte A, Verbeet MP, Brodniewicz-Proba T, Van Mourik JA, Mertens K. The interaction between human blood-coagulation factor VIII and von Willebrand factor. Characterization of a high-affinity binding site on factor VIII. *Biochem J.* 1989;257(3):679-683.
16. Vlot AJ, Koppelman SJ, van den Berg MH, Bouma BN, Sixma JJ. The affinity and stoichiometry of binding of human factor VIII to von Willebrand factor. *Blood.* 1995;85(11):3150-3157.
17. Dimitrov JD, Christophe OD, Kang J, et al. Thermodynamic analysis of the interaction of factor VIII with von Willebrand factor. *Biochemistry.* 2012;51(20):4108-4116.

18. Jorieux S, Gaucher C, Goudemand J, Mazurier C. A novel mutation in the D3 domain of von Willebrand factor markedly decreases its ability to bind factor VIII and affects its multimerization. *Blood*. 1998;92(12):4663-4670.
19. Hilbert L, Jorieux S, Proulle V, et al. Two novel mutations, Q1053H and C1060R, located in the D3 domain of von Willebrand factor, are responsible for decreased FVIII-binding capacity. *Br J Haematol*. 2003;120(4):627-632.
20. Mazurier C, Hilbert L. Type 2N von Willebrand disease. *Curr Hematol Rep*. 2005;4(5):350-358.
21. Castaman G, Giacomelli SH, Jacobi P, et al. Homozygous type 2N R854W von Willebrand factor is poorly secreted and causes a severe von Willebrand disease phenotype. *J Thromb Haemost*. 2010;8(9):2011-2016.
22. Chiu PL, Bou-Assaf GM, Chhabra ES, et al. Mapping the interaction between factor VIII and von Willebrand factor by electron microscopy and mass spectrometry. *Blood*. 2015;126(8):935-938.
23. Yee A, Oleskie AN, Dosey AM, et al. Visualization of an N-terminal fragment of von Willebrand factor in complex with factor VIII. *Blood*. 2015;126(8):939-942.
24. Przeradzka MA, van Galen J, Ebberink E, et al. D' domain region Arg782-Cys799 of von Willebrand factor contributes to factor VIII binding. *Haematologica*. 2020;105(6):1695-1703.
25. Fuller JR, Knockenhauer KE, Leksa NC, Peters RT, Batchelor JD. Molecular determinants of the factor VIII/von Willebrand factor complex revealed by BIVV001 cryo-electron microscopy. *Blood*. 2021;137(21):2970-2980.
26. Mazurier C, Goudemand J, Hilbert L, Caron C, Fressinaud E, Meyer D. Type 2N von Willebrand disease: clinical manifestations, pathophysiology, laboratory diagnosis and molecular biology. *Best Pract Res Clin Haematol*. 2001;14(2):337-347.
27. Swystun LL, Georgescu I, Mewburn J, et al. Abnormal von Willebrand factor secretion, factor VIII stabilization and thrombus dynamics in type 2N von Willebrand disease mice. *J Thromb Haemost*. 2017;15(8):1607-1619.
28. Shi Q, Fahs SA, Mattson JG, et al. A novel mouse model of type 2N VWD was developed by CRISPR/Cas9 gene editing and recapitulates human type 2N VWD. *Blood Adv*. 2022;6(9):2778-2790.
29. Bendetowicz AV, Morris JA, Wise RJ, Gilbert GE, Kaufman RJ. Binding of factor VIII to von willebrand factor is enabled by cleavage of the von Willebrand factor propeptide and enhanced by formation of disulfide-linked multimers. *Blood*. 1998;92(2):529-538.
30. Eikenboom JC, Castaman G, Kamphuisen PW, Rosendaal FR, Bertina RM. The factor VIII/von Willebrand factor ratio discriminates between reduced synthesis and increased clearance of von Willebrand factor. *Thromb Haemost*. 2002;87(2):252-257.
31. Whittaker CA, Hynes RO. Distribution and evolution of von Willebrand/integrin A domains: widely dispersed domains with roles in cell adhesion and elsewhere. *Mol Biol Cell*. 2002;13(10):3369-3387.
32. Lee JO, Rieu P, Arnaout MA, Liddington R. Crystal structure of the A domain from the alpha subunit of integrin CR3 (CD11b/CD18). *Cell*. 1995;80(4):631-638.

33. Celikel R, Varughese KI, Madhusudan, Yoshioka A, Ware J, Ruggeri ZM. Crystal structure of the von Willebrand factor A1 domain in complex with the function blocking NMC-4 Fab. *Nat Struct Biol.* 1998;5(3):189-194.
34. Emsley J, Cruz M, Handin R, Liddington R. Crystal structure of the von Willebrand Factor A1 domain and implications for the binding of platelet glycoprotein Ib. *J Biol Chem.* 1998;273(17):10396-10401.
35. Ruggeri ZM, Orje JN, Habermann R, Federici AB, Reininger AJ. Activation-independent platelet adhesion and aggregation under elevated shear stress. *Blood.* 2006;108(6):1903-1910.
36. Huizinga EG, Tsuji S, Romijn RA, et al. Structures of glycoprotein Ibalpha and its complex with von Willebrand factor A1 domain. *Science.* 2002;297(5584):1176-1179.
37. Dumas JJ, Kumar R, McDonagh T, et al. Crystal structure of the wild-type von Willebrand factor A1-glycoprotein Ibalpha complex reveals conformation differences with a complex bearing von Willebrand disease mutations. *J Biol Chem.* 2004;279(22):23327-23334.
38. Blenner MA, Dong X, Springer TA. Structural basis of regulation of von Willebrand factor binding to glycoprotein Ib. *J Biol Chem.* 2014;289(9):5565-5579.
39. Ju L, Dong JF, Cruz MA, Zhu C. The N-terminal flanking region of the A1 domain regulates the force-dependent binding of von Willebrand factor to platelet glycoprotein Ibalpha. *J Biol Chem.* 2013;288(45):32289-32301.
40. Tischer A, Cruz MA, Auton M. The linker between the D3 and A1 domains of vWF suppresses A1-GPIbalpha catch bonds by site-specific binding to the A1 domain. *Protein Sci.* 2013;22(8):1049-1059.
41. Deng W, Wang Y, Druzak SA, et al. A discontinuous autoinhibitory module masks the A1 domain of von Willebrand factor. *J Thromb Haemost.* 2017;15(9):1867-1877.
42. Arce NA, Cao W, Brown AK, et al. Activation of von Willebrand factor via mechanical unfolding of its discontinuous autoinhibitory module. *Nat Commun.* 2021;12(1):2360.
43. Arce NA, Markham-Lee Z, Liang Q, et al. Conformational activation and inhibition of von Willebrand factor by targeting its autoinhibitory module. *Blood.* 2024.
44. Girma JP, Takahashi Y, Yoshioka A, Diaz J, Meyer D. Ristocetin and botrocetin involve two distinct domains of von Willebrand factor for binding to platelet membrane glycoprotein Ib. *Thromb Haemost.* 1990;64(2):326-332.
45. Hulstein JJ, de Groot PG, Silence K, Veyradier A, Fijnheer R, Lenting PJ. A novel nanobody that detects the gain-of-function phenotype of von Willebrand factor in ADAMTS13 deficiency and von Willebrand disease type 2B. *Blood.* 2005;106(9):3035-3042.
46. Groot E, de Groot PG, Fijnheer R, Lenting PJ. The presence of active von Willebrand factor under various pathological conditions. *Curr Opin Hematol.* 2007;14(3):284-289.
47. Ulrichs H, Silence K, Schoolmeester A, et al. Antithrombotic drug candidate ALX-0081 shows superior preclinical efficacy and safety compared with currently marketed antiplatelet drugs. *Blood.* 2011;118(3):757-765.
48. Peyvandi F, Scully M, Kremer Hovinga JA, et al. Caplacizumab for Acquired Thrombotic Thrombocytopenic Purpura. *N Engl J Med.* 2016;374(6):511-522.

49. Chopek MW, Girma JP, Fujikawa K, Davie EW, Titani K. Human von Willebrand factor: a multivalent protein composed of identical subunits. *Biochemistry*. 1986;25(11):3146-3155.
50. Zhang Q, Zhou YF, Zhang CZ, Zhang X, Lu C, Springer TA. Structural specializations of A2, a force-sensing domain in the ultralarge vascular protein von Willebrand factor. *Proc Natl Acad Sci U S A*. 2009;106(23):9226-9231.
51. Jakobi AJ, Mashaghi A, Tans SJ, Huizinga EG. Calcium modulates force sensing by the von Willebrand factor A2 domain. *Nat Commun*. 2011;2:385.
52. Zhou M, Dong X, Baldauf C, et al. A novel calcium-binding site of von Willebrand factor A2 domain regulates its cleavage by ADAMTS13. *Blood*. 2011;117(17):4623-4631.
53. Lynch CJ, Lane DA, Luken BM. Control of VWF A2 domain stability and ADAMTS13 access to the scissile bond of full-length VWF. *Blood*. 2014;123(16):2585-2592.
54. Morioka Y, Casari C, Wohner N, et al. Expression of a structurally constrained von Willebrand factor variant triggers acute thrombotic thrombocytopenic purpura in mice. *Blood*. 2014;123(21):3344-3353.
55. Zanardelli S, Chion AC, Groot E, et al. A novel binding site for ADAMTS13 constitutively exposed on the surface of globular VWF. *Blood*. 2009;114(13):2819-2828.
56. Petri A, Kim HJ, Xu Y, et al. Crystal structure and substrate-induced activation of ADAMTS13. *Nat Commun*. 2019;10(1):3781.
57. Crawley JT, de Groot R, Xiang Y, Luken BM, Lane DA. Unraveling the scissile bond: how ADAMTS13 recognizes and cleaves von Willebrand factor. *Blood*. 2011;118(12):3212-3221.
58. Xu AJ, Springer TA. Mechanisms by which von Willebrand disease mutations destabilize the A2 domain. *J Biol Chem*. 2013;288(9):6317-6324.
59. Rayes J, Hommais A, Legendre P, et al. Effect of von Willebrand disease type 2B and type 2M mutations on the susceptibility of von Willebrand factor to ADAMTS-13. *J Thromb Haemost*. 2007;5(2):321-328.
60. Shim K, Anderson PJ, Tuley EA, Wiswall E, Sadler JE. Platelet-VWF complexes are preferred substrates of ADAMTS13 under fluid shear stress. *Blood*. 2008;111(2):651-657.
61. Cao W, Krishnaswamy S, Camire RM, Lenting PJ, Zheng XL. Factor VIII accelerates proteolytic cleavage of von Willebrand factor by ADAMTS13. *Proc Natl Acad Sci U S A*. 2008;105(21):7416-7421.
62. Van Belle E, Rauch A, Vincentelli A, et al. Von Willebrand factor as a biological sensor of blood flow to monitor percutaneous aortic valve interventions. *Circ Res*. 2015;116(7):1193-1201.
63. Van Belle E, Rauch A, Vincent F, et al. Von Willebrand Factor Multimers during Transcatheter Aortic-Valve Replacement. *N Engl J Med*. 2016;375(4):335-344.
64. Lankhof H, van Hoesel M, Schiphorst ME, et al. A3 domain is essential for interaction of von Willebrand factor with collagen type III. *Thromb Haemost*. 1996;75(6):950-958.
65. Huizinga EG, Martijn van der Plas R, Kroon J, Sixma JJ, Gros P. Crystal structure of the A3 domain of human von Willebrand factor: implications for collagen binding. *Structure*. 1997;5(9):1147-1156.

66. Bienkowska J, Cruz M, Atiemo A, Handin R, Liddington R. The von willebrand factor A3 domain does not contain a metal ion-dependent adhesion site motif. *J Biol Chem.* 1997;272(40):25162-25167.
67. Romijn RA, Westein E, Bouma B, et al. Mapping the collagen-binding site in the von Willebrand factor-A3 domain. *J Biol Chem.* 2003;278(17):15035-15039.
68. Lisman T, Raynal N, Groeneveld D, et al. A single high-affinity binding site for von Willebrand factor in collagen III, identified using synthetic triple-helical peptides. *Blood.* 2006;108(12):3753-3756.
69. Brondijk TH, Bihan D, Farndale RW, Huizinga EG. Implications for collagen I chain registry from the structure of the collagen von Willebrand factor A3 domain complex. *Proc Natl Acad Sci U S A.* 2012;109(14):5253-5258.
70. Ribba AS, Loisel I, Lavergne JM, et al. Ser968Thr mutation within the A3 domain of von Willebrand factor (VWF) in two related patients leads to a defective binding of VWF to collagen. *Thromb Haemost.* 2001;86(3):848-854.
71. Legendre P, Navarrete AM, Rayes J, et al. Mutations in the A3 domain of Von Willebrand factor inducing combined qualitative and quantitative defects in the protein. *Blood.* 2013;121(11):2135-2143.
72. Riddell AF, Gomez K, Millar CM, et al. Characterization of W1745C and S1783A: 2 novel mutations causing defective collagen binding in the A3 domain of von Willebrand factor. *Blood.* 2009;114(16):3489-3496.
73. Flood VH, Lederman CA, Wren JS, et al. Absent collagen binding in a VWF A3 domain mutant: utility of the VWF:CB in diagnosis of VWD. *J Thromb Haemost.* 2010;8(6):1431-1433.
74. Shida Y, Rydz N, Stegner D, et al. Analysis of the role of von Willebrand factor, platelet glycoprotein VI-, and alpha2beta1-mediated collagen binding in thrombus formation. *Blood.* 2014;124(11):1799-1807.
75. Santoro SA. Preferential binding of high molecular weight forms of von Willebrand factor to fibrillar collagen. *Biochim Biophys Acta.* 1983;756(1):123-126.
76. Bendetowicz AV, Wise RJ, Gilbert GE. Collagen-bound von Willebrand factor has reduced affinity for factor VIII. *J Biol Chem.* 1999;274(18):12300-12307.
77. Kizlik-Masson C, Peyron I, Gangnard S, et al. A nanobody against the VWF A3 domain detects ADAMTS13-induced proteolysis in congenital and acquired VWD. *Blood.* 2023;141(12):1457-1468.
78. Bork P. The modular architecture of a new family of growth regulators related to connective tissue growth factor. *FEBS Lett.* 1993;327(2):125-130.
79. Garcia Abreu J, Coffinier C, Larrain J, Oelgeschlager M, De Robertis EM. Chordin-like CR domains and the regulation of evolutionarily conserved extracellular signaling systems. *Gene.* 2002;287(1-2):39-47.
80. O'Leary JM, Hamilton JM, Deane CM, Valeyev NV, Sandell LJ, Downing AK. Solution structure and dynamics of a prototypical chordin-like cysteine-rich repeat (von Willebrand Factor type C module) from collagen IIA. *J Biol Chem.* 2004;279(51):53857-53866.

81. Zhang JL, Qiu LY, Kotsch A, et al. Crystal structure analysis reveals how the Chordin family member crossveinless 2 blocks BMP-2 receptor binding. *Dev Cell*. 2008;14(5):739-750.
82. Xu ER, Blythe EE, Fischer G, Hyvonen M. Structural analyses of von Willebrand factor C domains of collagen 2A and CCN3 reveal an alternative mode of binding to bone morphogenetic protein-2. *J Biol Chem*. 2017;292(30):12516-12527.
83. Xu ER, von Bulow S, Chen PC, et al. Structure and dynamics of the platelet integrin-binding C4 domain of von Willebrand factor. *Blood*. 2019;133(4):366-376.
84. Ruggeri ZM, De Marco L, Gatti L, Bader R, Montgomery RR. Platelets have more than one binding site for von Willebrand factor. *J Clin Invest*. 1983;72(1):1-12.
85. Pietu G, Chereil G, Marguerie G, Meyer D. Inhibition of von Willebrand factor-platelet interaction by fibrinogen. *Nature*. 1984;308(5960):648-649.
86. Lankhof H, Wu YP, Vink T, et al. Role of the glycoprotein Ib-binding A1 repeat and the RGD sequence in platelet adhesion to human recombinant von Willebrand factor. *Blood*. 1995;86(3):1035-1042.
87. Denis C, Williams JA, Lu X, Meyer D, Baruch D. Solid-phase von Willebrand factor contains a conformationally active RGD motif that mediates endothelial cell adhesion through the alpha v beta 3 receptor. *Blood*. 1993;82(12):3622-3630.
88. Konig G, Obser T, Marggraf O, et al. Alteration in GPIIb/IIIa Binding of VWD-Associated von Willebrand Factor Variants with C-Terminal Missense Mutations. *Thromb Haemost*. 2019;119(7):1102-1111.
89. Legendre P, Delrue M, Boisseau P, et al. Functional study of two mutations in the C4 domain of von Willebrand factor. *J Thromb Haemostas*. 2015;13(S2):748.
90. Marx I, Christophe OD, Lenting PJ, et al. Altered thrombus formation in von Willebrand factor-deficient mice expressing von Willebrand factor variants with defective binding to collagen or GPIIbIIIa. *Blood*. 2008;112(3):603-609.
91. Navarrete AM, Casari C, Legendre P, et al. A murine model to characterize the antithrombotic effect of molecules targeting human von Willebrand factor. *Blood*. 2012;120(13):2723-2732.
92. Veyradier A, Jumilly AL, Ribba AS, et al. New assay for measuring binding of platelet glycoprotein IIb/IIIa to unpurified von Willebrand factor. *Thromb Haemost*. 1999;82(1):134-139.
93. Fu H, Jiang Y, Yang D, Scheiflinger F, Wong WP, Springer TA. Flow-induced elongation of von Willebrand factor precedes tension-dependent activation. *Nat Commun*. 2017;8(1):324.
94. Bergal HT, Jiang Y, Yang D, Springer TA, Wong WP. Conformation of von Willebrand factor in shear flow revealed with stroboscopic single-molecule imaging. *Blood*. 2022;140(23):2490-2499.
95. Savage B, Sixma JJ, Ruggeri ZM. Functional self-association of von Willebrand factor during platelet adhesion under flow. *Proc Natl Acad Sci U S A*. 2002;99(1):425-430.
96. Fu H, Jiang Y, Wong WP, Springer TA. Single-molecule imaging of von Willebrand factor reveals tension-dependent self-association. *Blood*. 2021;138(23):2425-2434.
97. Chung DW, Platten K, Ozawa K, et al. Low-density lipoprotein promotes microvascular thrombosis by enhancing von Willebrand factor self-association. *Blood*. 2023;142(13):1156-1166.

98. Chung DW, Chen J, Ling M, et al. High-density lipoprotein modulates thrombosis by preventing von Willebrand factor self-association and subsequent platelet adhesion. *Blood*. 2016;127(5):637-645.
99. Zhang C, Kelkar A, Neelamegham S. von Willebrand factor self-association is regulated by the shear-dependent unfolding of the A2 domain. *Blood Adv*. 2019;3(7):957-968.
100. Adam F, Casari C, Prevost N, et al. A genetically-engineered von Willebrand disease type 2B mouse model displays defects in hemostasis and inflammation. *Sci Rep*. 2016;6:26306.

Figure 1

Figure 1

VWF domain structure

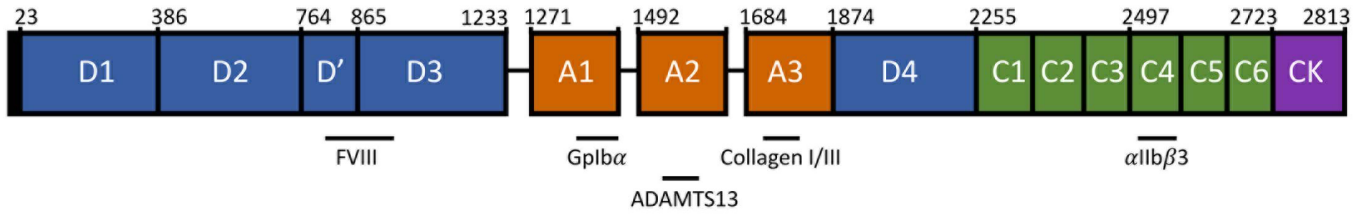


Figure 2

Figure 2

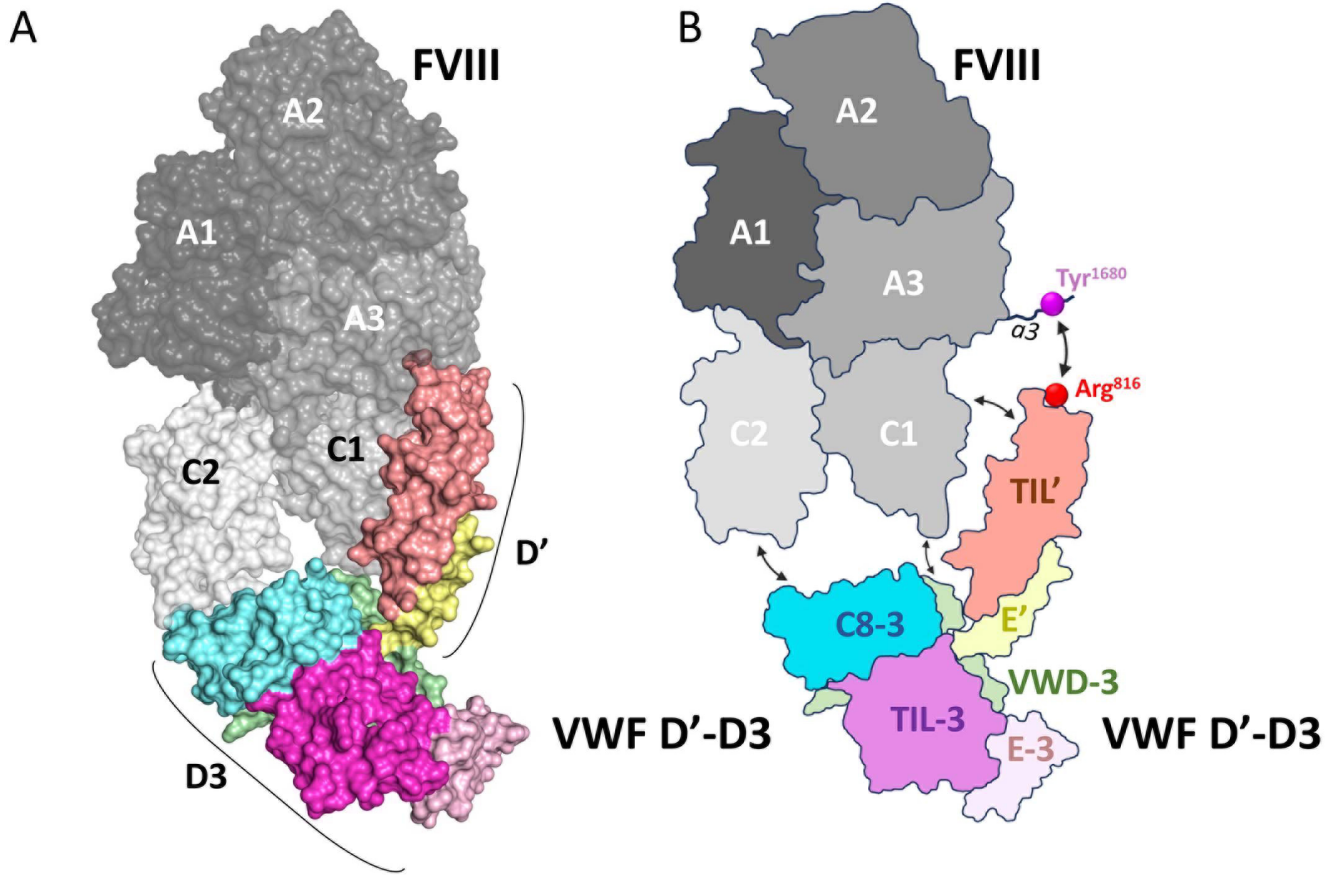


Figure 3

Figure 3

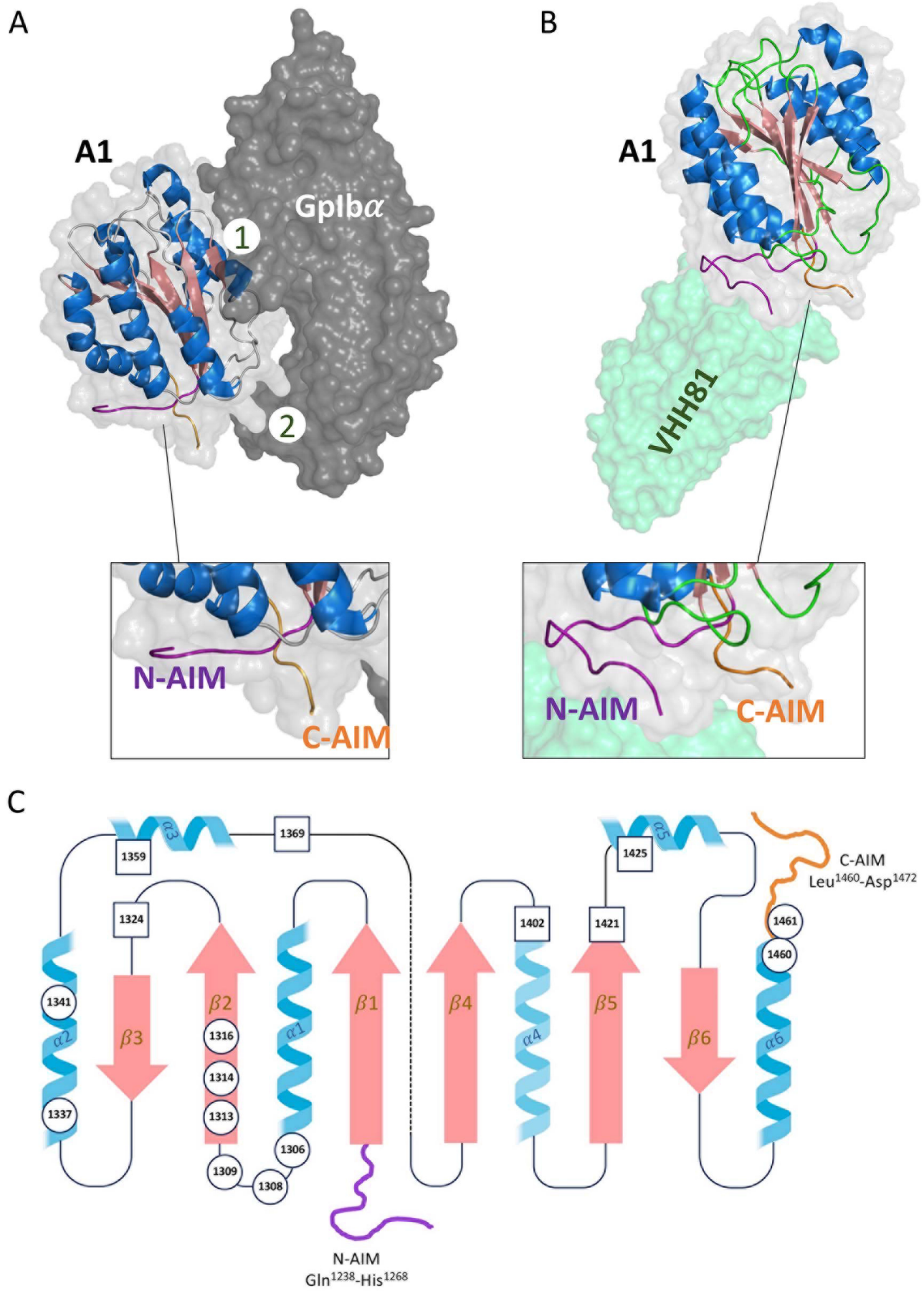


Figure 4

Figure 4

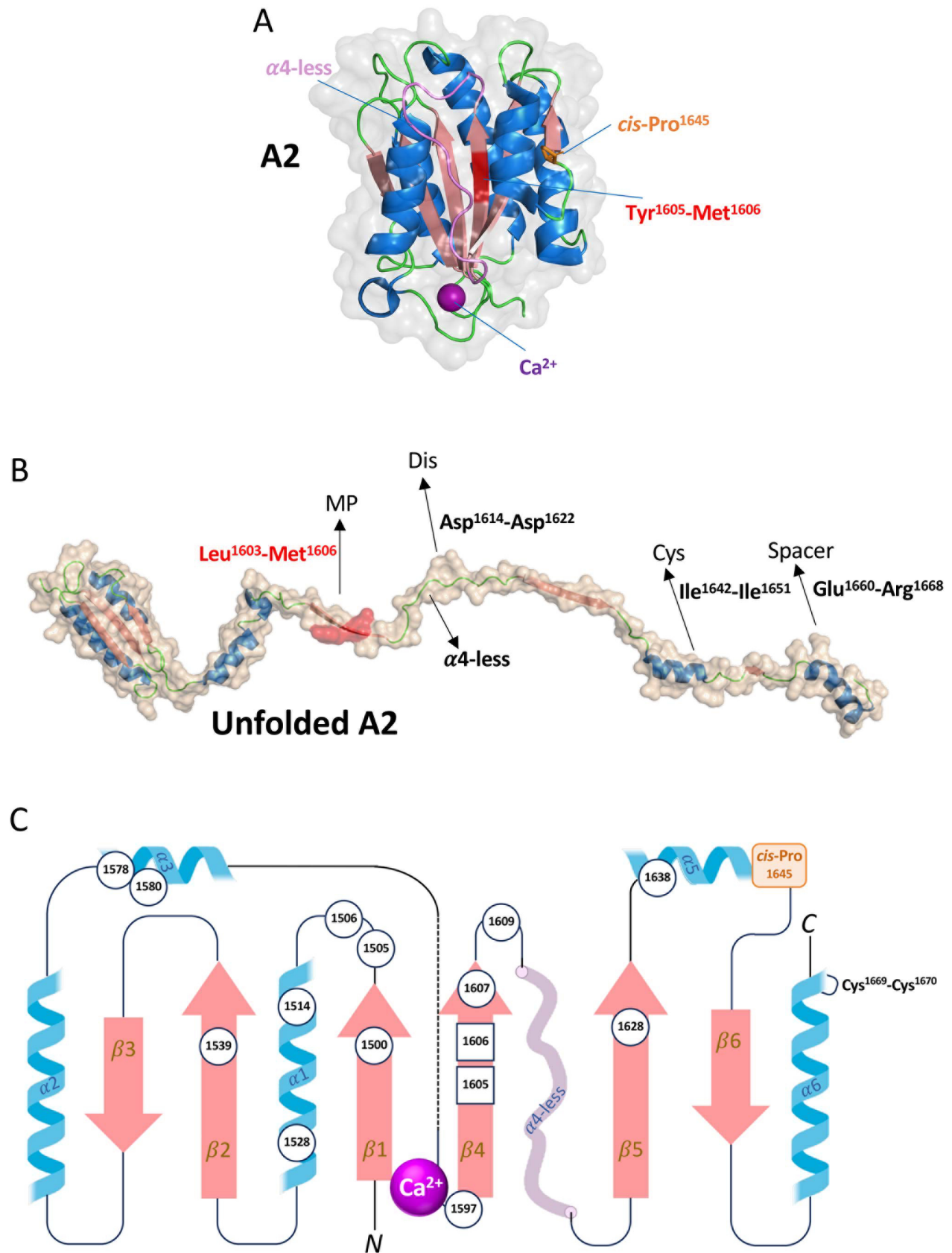


Figure 5

Figure 5

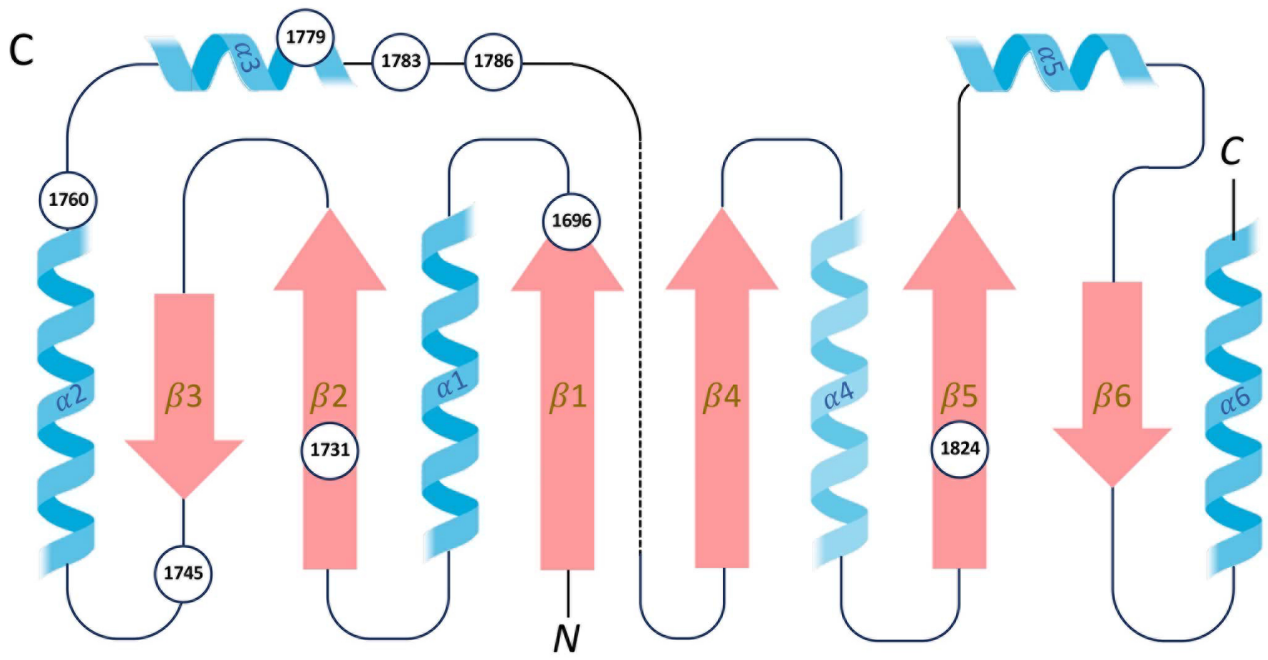
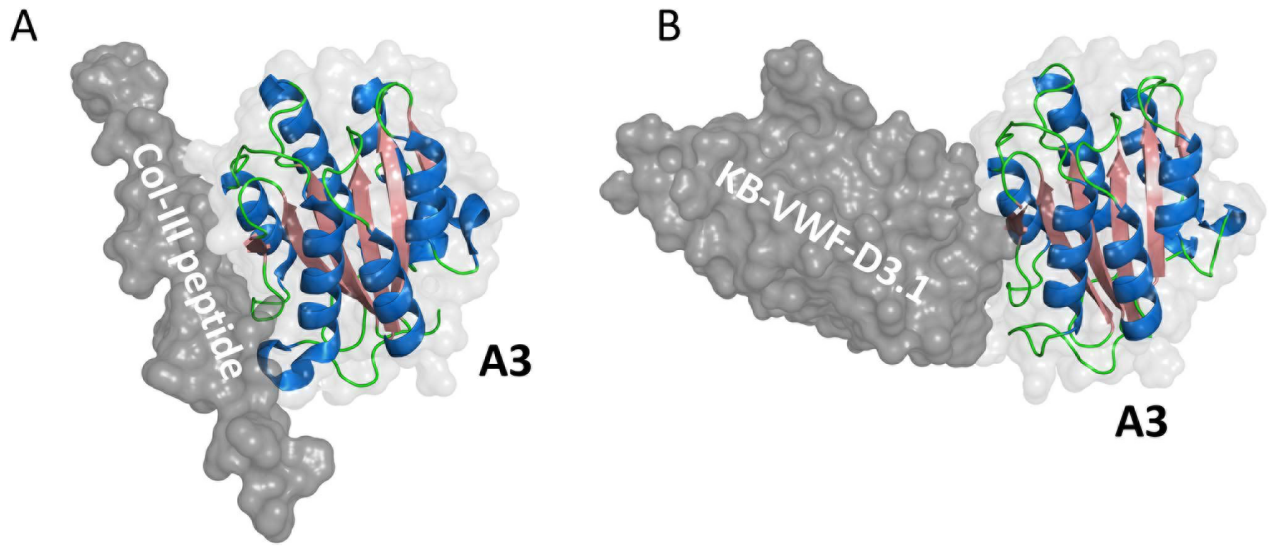


Figure 6

Figure 6

